Journal of Computer-Aided Molecular Design, 8 (1994) 223–230
ESCOM

J-CAMD 245

Design of potential angiogenin inhibitors

B.J. Howlin*, N.P. Tomkinson, J. Chen and G.A. Webb

Department of Chemistry, University of Surrey, Guildford, Surrey GU2 5XH, U.K.

Received 1 September 1993
Accepted 6 December 1993

Key words: Angiogenin; TAN1120; Homology; Ribonuclease A

SUMMARY

A model of angiogenin has been prepared by homology modelling, based upon the structure of ribonuclease A. This model has been used to postulate an inhibitor based upon the angiostatic agent TAN1120. The complex of ribonuclease A with a dinucleotide has been modelled and used as a guide to the binding orientation of daunomycin – the closest TAN1120 analogue for which the crystal structure and stereochemistry are available.

INTRODUCTION

Angiogenin is a small (123 residues) extracellular protein that induces blood vessel formation [1]. Angiogenin has 36% homology and 56% sequence similarity with pancreatic ribonuclease A. The active site is conserved in the alignment, as are three out of the four disulfide bridges. Angiogenin is also ribonucleolytic, although the specificities of the two enzymes are very different, with angiogenin being specific for large (1000–5000 bases) oligonucleotides [2]. The angiogenic activity of angiogenin depends upon whether or not it has an intact active site [3].

Although essential for normal growth and repair of tissues, angiogenesis can be pathological when uncontrolled, as seen in tumour growth and diabetic retinopathy [4]. Inhibition of angiogenin and thereby of angiogenesis has great therapeutic potential and an obvious approach to this goal is to design mimics of the natural substrate. The minimal substrate for ribonuclease is a 2'-3' cyclic nucleotide. More relevant to nucleotide cleavage, the second smallest substrate is a dinucleotide. A 1989 patent described an angiostatic agent, isolated from *Streptomyces triangulatus*, called TAN1120 [5]. The mechanism of angiogenesis inhibition by TAN1120 is unknown, but it may involve DNA intercalation, bearing in mind the similarity of TAN1120 to daunomycin (Fig. 1). An alternative mechanism of action, based upon a structural similarity to a dinucleotide, involves TAN1120 binding to angiogenin. A number of structural and chemical

*To whom correspondence should be addressed.

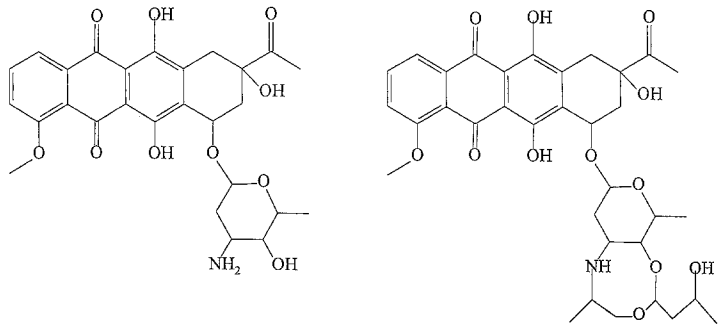

Fig. 1. Structures of (left) daunomycin and (right) TAN1120.

features of a dinucleotide are reproduced in the TAN1120 structure (Fig. 2). The present modelling study aims to provide evidence that TAN1120 will bind to angiogenin, reinforcing the hypothesis that TAN1120 is an inhibitor of angiogenin.

There is no available crystal or NMR structure for angiogenin (although crystals have recently been prepared and a preliminary X-ray analysis performed [6]). In addition, no structural data are available for ribonuclease A–dinucleotide complexes and so the preliminary steps involve modelling these structures. With a model of angiogenin and a model of the ribonuclease A–dinucleotide complex, it is possible to proceed by modelling daunomycin – the closest analogue of TAN1120 for which crystal and stereochemical data are available – at the active sites of ribonuclease A and angiogenin and to derive additional functionality for the ligand, based upon the complexed structures.

MATERIALS AND METHODS

All calculations were performed on a Silicon Graphics 4D/20 personal Iris workstation and a Silicon Graphics Indigo R3000. CHARMm version 21.3 [7] was used for all the molecular mechanics calculations and the sequence alignment and model building were performed using the modelling package QUANTA 3.0 by Polygen. The united atom representation was used for the protein, i.e., only hydrogens in polar groups were modelled explicitly. The following nonbonded

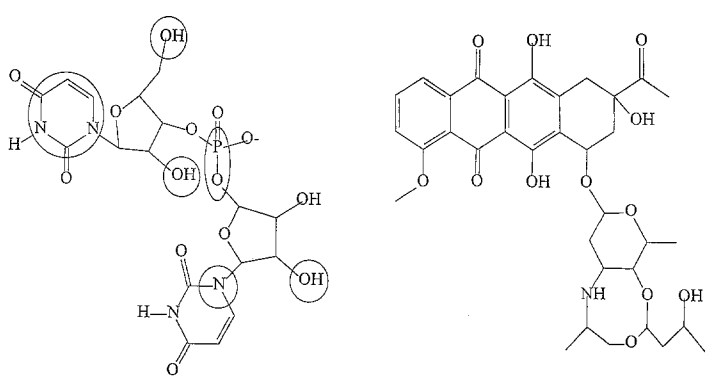

Fig. 2. Two-dimensional comparison of a uridyl-uridine and TAN1120, showing common structural features (circled).

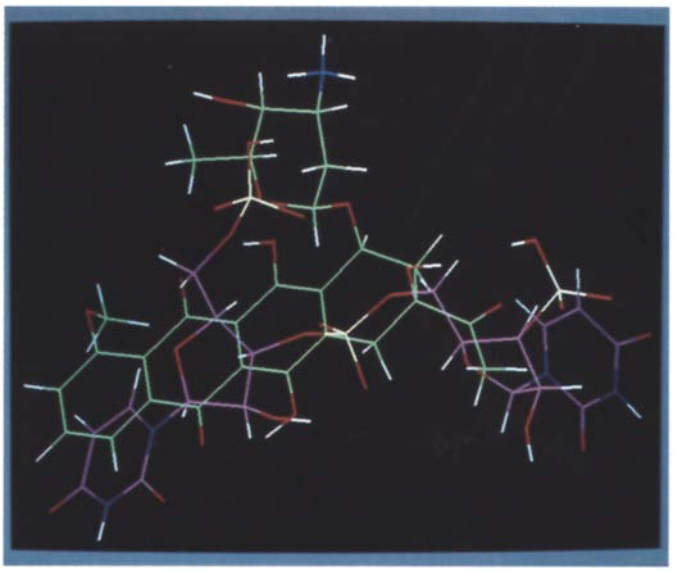

Fig. 3. The orientation of daunomycin (green) that produced the best Dock force field score (lowest intermolecular potential energy) within the angiogenin active site, superimposed upon the structure of uridyl-uridine (purple) from which the sphere centres were derived for the docking procedure. By comparison with the postulated analogy shown in Fig. 2, daunomycin is inverted and the amino sugar does not correspond with the ribose of the 3'-uridine.

scheme was used: nonbonded update every 10 steps, 14.0 Å van der Waals and electrostatic cutoff shifted over 8–12 Å, distance-dependent dielectric, dielectric constant of 1.0. The adopted basis-set Newton Raphson (ABNR) energy minimisation algorithm and Verlet constant-energy molecular dynamics were used throughout.

The structure of angiogenin was modelled upon the coordinates of bovine pancreatic ribonuclease A [8], entry 3rn3, obtained from the Protein Data Bank [9,10]. A model was built previously by Palmer et al. [11], but with fixed bond lengths and angles. All degrees of freedom were included in the current procedure. Small side chains with poor contacts were spun automatically in 30° increments, larger side chains (arginine, lysine) were modelled manually to remove close

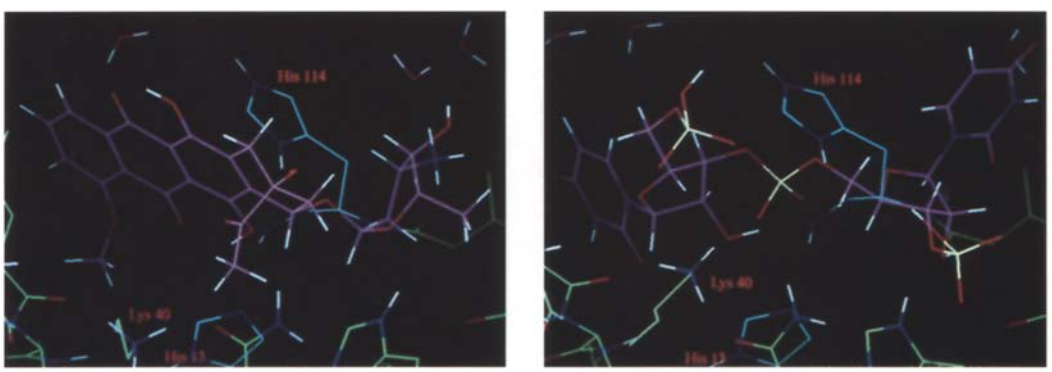

Fig. 4. Left: dinucleotide complex with angiogenin; right: daunomycin complex with angiogenin. His^{114} is directly above and His^{13} directly below the ligand.

contacts and maximise hydrogen bonding. Deletions were regularised (energy minimised with constraints on the rest of the protein). Residues 1–3 (angiogenin numbering) were left with no secondary structure, while residues 119–123 were predicted to be helical using the Chou and Fassman rules [12] and were modelled as such. Crystallographic waters and the sulfate ion at the active site were transferred from the ribonuclease structure and added to the rough angiogenin structure. The active-site histidines 13 and 114 in angiogenin both have pKa values in the range 5–8 and hence will be freely exchanging at physiological pH. Therefore, as the postulated mechanism for ribonuclease A assumes His^{114} protonated and His^{13} neutral, we have taken this as the protonation state of these residues. The structure was then refined using constrained molecular dynamics. Tight harmonic constraints (50 kcal/mol $Å^2$) were applied to the backbone atoms and to the conserved amino acid side chains. The protein was then subjected to molecular dynamics for 20 ps at a simulated temperature of 800 K, using a time step of 1 fs. Heating was performed over 4 ps, with assignment of velocities from a Gaussian distribution, and equilibration over 5 ps at 800 K, with scaling of velocities by a single factor every 100 fs to keep the temperature within a window of ± 10 K. The constraints were then removed during subsequent energy minimisation.

The refined structure was analysed using the program Procheck [13]. This provides a graphic representation of the main-chain dihedral angles (Ramachandran plot) and of the two side-chain dihedral angles closest to the main chain (χ^1/χ^2). Two residues (Asn^{109}, Tyr^{25}) were found in disallowed regions of the Ramachandran plot compared to the ribonuclease crystal structure, which had none in these regions. However, the χ^1/χ^2 plot showing the quality of the side-chain placements was significantly better for the angiogenin model, with only six residues significantly deviating from gauche/anti conformations as compared to 12 residues for ribonuclease A.

The structure of uridyl-uridine–ribonuclease A was prepared from the crystal structure of uridine vanadate–ribonuclease A [14], entry 6rsa, obtained from the Protein Data Bank [9,10]. It is assumed that any stretch of oligonucleotide that is hydrolysed by ribonuclease A will consist of repeating units with the same or similar conformation, and so it is appropriate to use the uridine ligand already present at the B_1 subsite in the crystal structure as the conformation for docking to the B_2 subsite. To this end, the uridine vanadate ligand was extracted from the active site of the protein and converted to uridine 3'-monophosphate (3'-UMP). This was energy minimised in vacuo using the aforementioned nonbonding scheme. This structure was then docked at the active site of uridine vanadate–ribonuclease A. The Dock 3.0 [15] procedure was used for all automated docking. Dock generates a large number of orientations of the ligand at the active site of the protein and then scores them according to the energies of a van der Waals plus Coulombic interaction of the ligand with a grid of points representing the protein. Thus, orientations with low intermolecular nonbonded potential energies score highly. CHARMm charges were used for the ligand and the protein. The recommended default parameters were used for Dock, i.e., a dielectric of 1/r where r is the distance between the two atoms in the Coulombic interaction, with the exception that a grid with dimensions 27.404 × 29.756 × 18.995 Å and grid spacing of 0.31 Å (the smallest spacing available for such a large grid) was generated. This grid spans both the B_1 and B_2 subsites of ribonuclease A.

A total of 107 orientations of 3'-UMP at the active site of uridine–ribonuclease A with intermolecular potential energies less than –10 kcal/mol were generated. The orientation with the lowest intermolecular potential energy (best force field score, –21.116 kcal/mol) was not consistent with the growing consensus as to the orientation of the B_2 base. Crystallographic studies (see

Pares et al. for a review [16]) suggest that the B_2 subsite is bounded by Gln^{69}, Asn^{71} and Glu^{111}. This is not the case with the highest scoring orientation found here. The base is orthogonal to this pocket, pointing away from the active-site histidines. The second best scoring orientation (worse by 0.9 kcal/mol) does, however, conform to the standard model. This orientation was accepted, as the approximations inherent in the docking procedure do not warrant an alternative binding mode being proposed without additional data. A phosphodiester bond was formed between the docked uridine and the ligand already present to give uridyl-uridine–ribonuclease A. This complex was energy minimised with harmonic constraints on the protein backbone (1.0 kcal/mol Å^2), on the crystallographic waters (0.1 kcal/mol Å^2) and on the crystallographic uridine and the sugar of the docked uridine (1.0 kcal/mol Å^2) during initial energy minimisation, to allow poor contacts to be relieved without disturbing the structure unnecessarily. These constraints were removed prior to final energy minimisation. The dinucleotide was then transferred to the active site of angiogenin, where it was energy minimised again. Certain residues impinging upon the active site were modified to give different rotamers prior to energy minimisation (Arg^5, Ile^{42}, Arg^{66}, Glu^{67} and Glu^{108}). The structure of uridyl-uridine–angiogenin was used as the basis for docking daunomycin.

The dinucleotide was removed from the active site for the docking of daunomycin. The heavy atoms from the dinucleotide were used as sphere centres in the input to the Dock procedure. First a molecular dynamics conformational search procedure was undertaken on the daunomycin molecule to generate an ensemble of low-energy structures. The crystal structure of daunomycin [17] was energy minimised, with charges calculated using the charge templates option within QUANTA. Daunomycin was then subjected to molecular dynamics for 1 ns at a simulated temperature of 1000 K, quenching every picosecond to give 1000 structures, which were then clustered according to an rms torsion angle deviation of 15°. This gave 103 structures with potential energies within 10 kcal/mol of the lowest energy structure. These 103 structures were all docked into the angiogenin active site. In this way 1097 orientations were generated. The lowest energy (best scoring, −26.525 kcal/mol) orientation was inverted with respect to the expected orientation, based upon the comparison shown in Fig. 2 – see Fig. 3. The lowest energy structure consistent with Fig. 2 had a force field score of −23.547 kcal/mol. An attempt was made to refine this structure further, using 50 ps of molecular dynamics at 500 K with harmonic constraints on the protein backbone (5.0 kcal/mol Å^2), on other protein atoms (0.5 kcal/mol Å^2), on water molecules (0.5 kcal/mol Å^2) and on the heavy atoms of the daunomycin tetracycle (5.0 kcal/mol Å^2). The structure was quenched every picosecond, using a short (100 cycles) energy minimisation, and the lowest energy structure was found to be the starting structure, indicating that the conformational space searched within this practicable amount of time did not contain any lower energy conformations. However, this also suggests that the structure is not trapped in an inaccessibly high energy state, unless the potential well is very deep.

RESULTS AND DISCUSSION

Figure 4 shows two structures, the daunomycin–angiogenin structure, and the dinucleotide uridyl-uridine–angiogenin structure, obtained by the modelling procedure discussed above. The central phosphate of the dinucleotide is shown positioned above the catalytic histidines. The left-hand (5') nucleotide is the one derived from the crystallographic coordinates of the uridine–

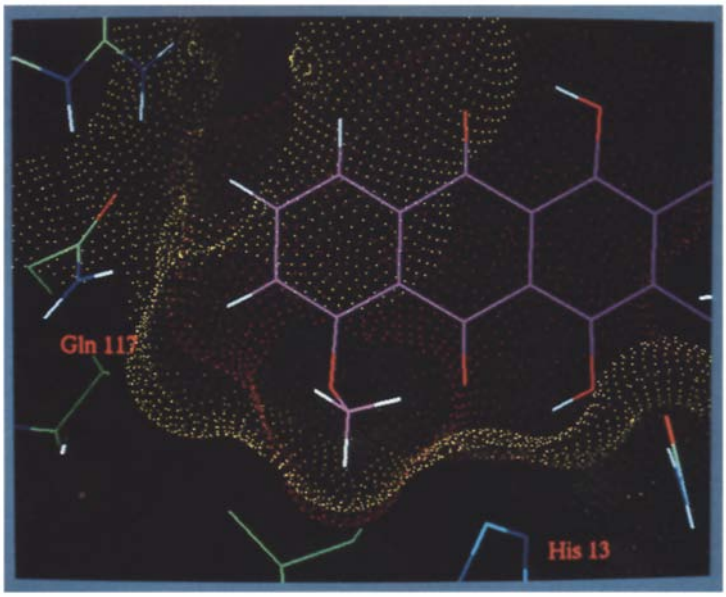

Fig. 5. Daunomycin bound to angiogenin, including a Connolly surface on the enzyme (yellow) and the ligand (red).

vanadate complex, the right-hand (3') one from docking. The daunomycin molecule adopts roughly the same orientation in the active site of angiogenin as does the dinucleotide. The amino sugar of daunomycin is in the same position as the 3'-end sugar of the dinucleotide. The terminal aromatic ring of the tetracycle adopts a similar position to the 5' base. In daunomycin, the central tetrahedral phosphate of the dinucleotide is replaced by one of the tetrahedral carbons of the

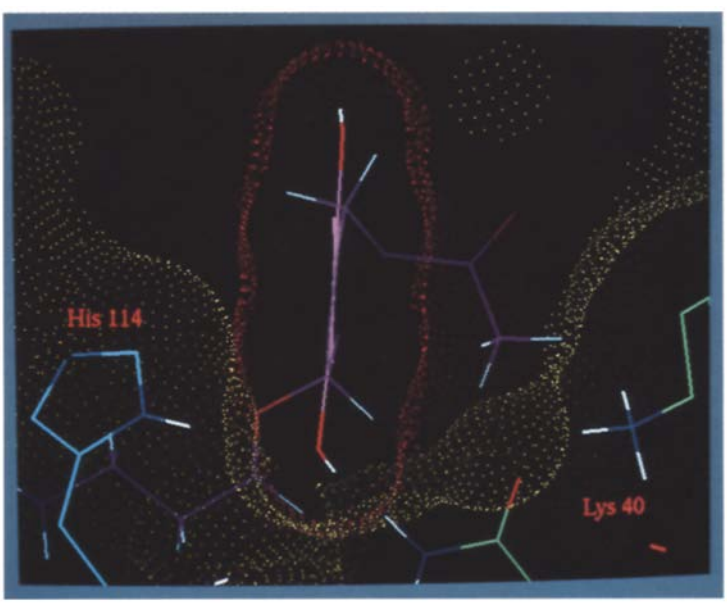

Fig. 6. An orthogonal view of the daunomycin–angiogenin complex shown in Fig. 5.

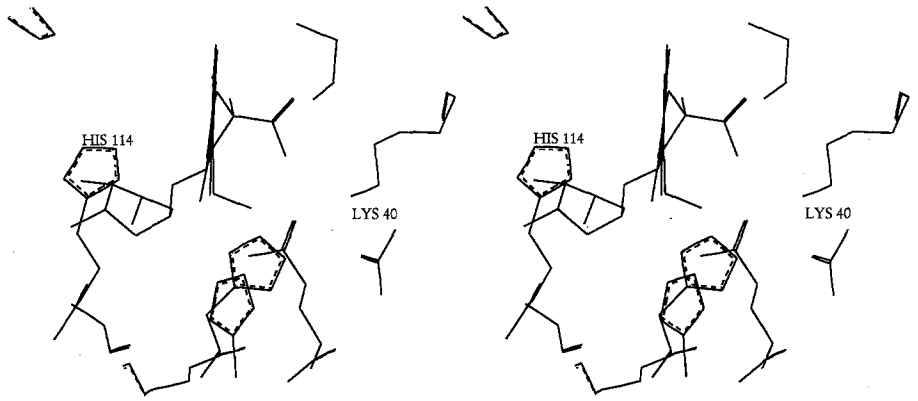

Fig. 7. Stereoview of the active site of angiogenin with daunomycin docked.

aliphatic ring of the tetracycle; the ether oxygen between the tetracycle and the amino sugar is in a position to hydrogen bond to the hydrogen attached to the N^{δ} of His^{114}. As such, daunomycin fits well in the pocket and provides a sterically restrained dinucleotide mimic. This provides support for the contention that daunomycin and TAN1120 bind to angiogenin.

Figures 5 and 6 show details of daunomycin docked at the active site of angiogenin with a Connolly surface superimposed. Figure 7 presents a black-and-white stereoview of this interaction. Figure 5 shows that there is room for additional functionality on the phenolic ring of the tetracycle – possibly an acidic group interacting with Lys^{40}. The upper hydroxyl group of the phenolic ring might be replaced by an anionic species to mimic the phosphate group of the dinucleotide (see Fig. 4). Figure 6 shows an orthogonal view of the same structure. Gln^{117} is replaced by alanine in ribonuclease A. Conversion of the terminal aromatic ring of the tetracycle to a lactam might provide a specific binding interaction with the glutamine. This would also increase the similarity to a uridine base. (The actual arrangement of the amide group might not be crucial, as glutamine can rotate 180° to reverse its orientation.) Room is also available for additional functionality, either on the pendant methoxy group or on the adjacent aromatic carbon. Alternatively, a fifth ring could be added to the tetracycle to fill this space. Upon these and

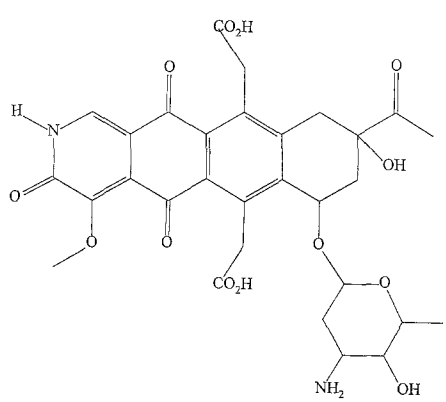

Fig. 8. A derivative of daunomycin with potential as a ligand for angiogenin. A lactam has been introduced and the phenolic hydroxyl groups have been replaced by carboxylic acid functionalities.

other potential modifications, improvements in binding can be based. The sugar has not been included in this discussion, simply because not enough is known about the stereochemistry of the eight-membered ring present in TAN1120 to model this region.

CONCLUSIONS

Models of angiogenin, angiogenin–dinucleotide complex and daunomycin–angiogenin complex have been generated and refined. It has been shown that daunomycin is a plausible ligand for angiogenin and by analogy TAN1120 should also be. There is as yet no experimental evidence for the binding of either TAN1120 or daunomycin to members of the ribonuclease superfamily, although their ED_{50} values against angiogenesis are known. Preliminary binding studies are being undertaken in this regard. The angiogenin–daunomycin complex structure is currently being used to design inhibitors of angiogenesis as improvements on the known inhibitor TAN1120. Potential areas of improvement have been highlighted and are represented in the derivative of daunomycin shown in Fig. 8.

ACKNOWLEDGEMENTS

We should like to thank the Association for International Cancer Research for funding and The Chemistry Department, The University, Newcastle upon Tyne for the kind use of computational facilities.

REFERENCES

1 Fett, J.W., Strydon, D.J., Lobb, R.R., Alderman, E.M., Bethume, J.L., Riordan, J.F. and Vallee, B.L., Biochemistry, 24 (1985) 5480.
2 Shapiro, R., Riordan, J.F. and Vallee, B.L., Biochemistry, 25 (1986) 3527.
3 Shapiro, R. and Vallee, B.L., Biochemistry, 28 (1989) 7401.
4 Klagsbrun, M. and D'Amore, P.A., Annu. Rev. Physiol., 53 (1991) 217.
5 Kanamaru, T., Nozaki, Y. and Masayuki, M., European Patent Application No. 89123719, 1989.
6 Acharya, K.R., Subramanian, V., Shapiro, R., Riordan, J.F. and Vallee, B.L., J. Mol. Biol., 228 (1992) 1269.
7 Brooks, B.R., Bruccoleri, R.E., Olafson, B.D., States, D.J., Swaminathan, S. and Karplus, M., J. Comput. Chem., 4 (1983) 8234.
8 Howlin, B.J., Harris, G.W., Moss, D.S. and Palmer, R.A., Brookhaven Data Bank entry 3rn3, Acta Crystallogr., A45 (1989) 851.
9 Abola, E.E., Bernstein, F.C., Bryant, S.H., Koetzle, T.F. and Weng, J., In Allen, F.H., Bergerhoff, G. and Sievers, R. (Eds.) Crystallographic databases – Information Content, Software Systems, Scientific Applications, Data Commission of the International Union of Crystallography, Cambridge, 1987, pp. 107–132.
10 Bernstein, F.C., Koetzle, T.F., Williams, G.J.B., Meyer Jr., E.F., Brice, M.D., Rodgers, J.R., Kennard, O., Shimanouchi, T. and Tasumi, M., J. Mol. Biol., 112 (1977) 535.
11 Palmer, K.A., Scheraga, H.A., Riordan, J.F. and Vallee, B.L., Proc. Natl. Acad. Sci. USA, 83 (1986) 1965.
12 Chou, P.Y. and Fasman, G.D., Adv. Enzymol., 47 (1978) 45.
13 Laskowski, R.A., MacArthur, M.W., Moss, D.S. and Thornton, J.M., J. Appl. Crystallogr., 26 (1993) 283.
14 Borah, B., Chen, C.-W., Egan, W., Miller, M., Wlodawer, A. and Cohen, J.S., Biochemistry, 24 (1985) 2058.
15 Meng, E.C., Shoichet, B.K. and Kuntz, I.D., J. Comput. Chem., 13 (1992) 505.
16 Pares, X., Nogues, M.V., De Lorens, R. and Cuchillo, C.M., Essays Biochem., 26 (1991) 89.
17 Courseilles, C., Busetta, B., Geoffre, S. and Hospital, M., Acta Crystallogr., B35 (1979) 764.